

Cite this: *RSC Adv.*, 2019, 9, 11365

Received 4th January 2019

Accepted 27th March 2019

DOI: 10.1039/c9ra00063a

rsc.li/rsc-advances

# Spontaneous formation and reversible transformation between achiral J- and chiral H-aggregates of cyanine dye MTC†

Ai-Jiao Guan,<sup>a</sup> Jing-Tao Zhang,<sup>a</sup> Li-Xia Wang,<sup>b</sup> Jie Cui,<sup>b</sup> Jun-Feng Xiang,<sup>b</sup> Xin Sun,<sup>a</sup> Kuo Chen,<sup>a</sup> Qian Li<sup>a</sup> and Ya-Lin Tang<sup>c</sup>

Chirality at a supramolecular level is currently attracting great attention attributed to rapid developments in supramolecular chemistry. Herein, we report a new type of chiral self-assembly based on the cyanine dye MTC. The chiral H-aggregates of MTC could form spontaneously from achiral J-aggregates, and could return back to achiral J-aggregates in high concentration on increasing the solution temperature.

The origin of optical activity on earth has been a major topic of interest in the scientific community. There are many chiral substances in nature, ranging from chiral drugs, biomacromolecules, and supramolecular systems, to microbes with spiral viruses, larger biological species such as snails, and even larger galaxies.<sup>1</sup> The concept of molecular chirality has long been recognized and provided guidance in the application of drugs and functional materials, while supramolecular chirality has attracted great attention in recent years.<sup>2</sup> Supramolecular chirality can be regarded as chirality at a supramolecular level in supramolecular chemistry, and is strongly related to self-assembly connected by non-covalent bonds. Molecular self-assembly plays an important role in supramolecular systems, which may process supramolecular chirality.<sup>3</sup> Chiral induction is the main source of chirality for supramolecular self-assembly, for example a main way of constructing and regulating chiral supramolecules is using biomolecules such as proteins, polypeptides, and duplex DNAs as templates.<sup>4</sup> The introduction of chiral molecules into achiral construction units and thus the new formation of self-assemblies leads to chiral signals.

In fact completely achiral molecules can also self-assemble into chiral supramolecular systems, which is defined as spontaneous symmetry breaking. Asymmetric environments between different interfaces are necessary for symmetry breaking, thus led to chiral liquid crystals, micelles, gel systems, LB films and so on.<sup>1</sup> However, there are only a few published reports of the

aggregation of achiral cyanine molecules in solution to form supramolecular chirality.<sup>5</sup> To our knowledge, the first paper on this issue was published in 1996, Dähne and co-workers found hydrophobic interaction between long alkyl chains of organic dyes played an important role in inducing the achiral molecules to undergo J-aggregates with supramolecular chirality.<sup>6</sup> In this manuscript we found cy3 dye MTC,<sup>7</sup> 3,3'-di(3-sulfopropyl)-4,5,4',5'-dibenzo-9-methyl-thiacarbocyanine triethylammonium salt, without long alkyl chains could lead to the formation of chiral H-aggregates. And the chiral H-aggregates was converted from achiral J-aggregates, and they are reversible in a certain temperature range. Further the formation of chiral H-aggregates was dependent on the concentration of alkali salts.

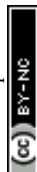
Cyanine dyes known as the oldest classes of synthetic compounds,<sup>8</sup> have shown a great tendency to self-associate, and find numerous applications in a variety of fields.<sup>9</sup> The different aggregates of cyanine dyes can be distinguished by UV/Vis spectroscopy, for example, H-aggregates is blue-shifted absorption band and J-aggregates is red-shifted absorption band, relative to monomer state.<sup>10</sup> As is known, MTC (Fig. 1) prefers to form H-aggregates with  $\lambda = 514$  nm in pure water,<sup>11</sup> which didn't show chiral signal by CD spectra. And by adding chloride salts into the above solution of MTC H-aggregates, which can transform into J-aggregates gradually.<sup>12</sup> However in our research, we found that 200  $\mu$ M MTC methanol solution was treated with 30 mM NaCl aqueous solution in the volume ration of 1 : 1, leading to the formation of chiral MTC H-aggregates. When the above solution was diluted to 5  $\mu$ M, the H-aggregates was characterized by UV/Vis spectra with the appearance of  $\lambda = 479$  nm and  $\lambda = 446$  nm (Fig. 1a and 2a), exhibiting distinct changes of blue shifted signals in the absorption band as compared to the monomeric state of  $\lambda = 583$  nm in methanol solution. The chiral feature of new formed H-aggregates was found by CD spectra, and it showed obviously strong molar ellipticity at room temperature.

<sup>a</sup>National Laboratory for Molecular Sciences, Center for Molecular Sciences, State Key Laboratory for Structural Chemistry of Unstable and Stable Species, Institute of Chemistry Chinese Academy of Sciences, Beijing 100190, China. E-mail: wlx8225@iccas.ac.cn; tangyl@iccas.ac.cn; Fax: +8610-82617304

<sup>b</sup>Center for Physicochemical Analysis and Measurement, Institute of Chemistry Chinese Academy of Sciences, Beijing 100190, China

<sup>c</sup>University of the Chinese Academy of Sciences, Beijing, 100049, China

† Electronic supplementary information (ESI) available. See DOI: 10.1039/c9ra00063a



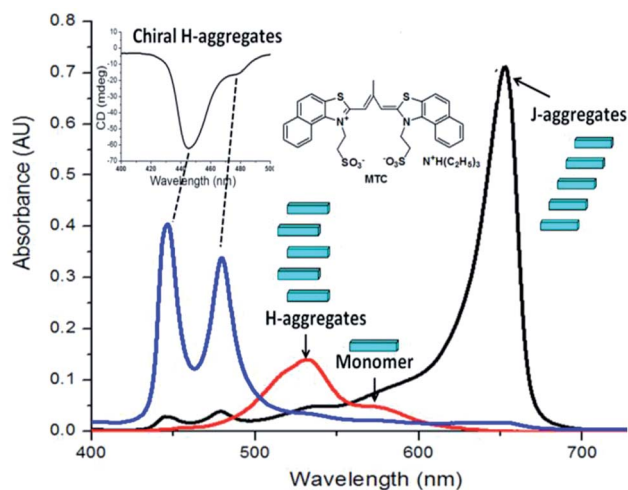


Fig. 1 The absorption spectra of 5  $\mu\text{M}$  MTC in different states.

In our studied system, we found that achiral J-aggregates in 100  $\mu\text{M}$  are firstly formed, and the solution color presents purple. At room temperature, the color of solution changes from purple to orange in 2 h (Fig. 2c), and the orange solution corresponds to

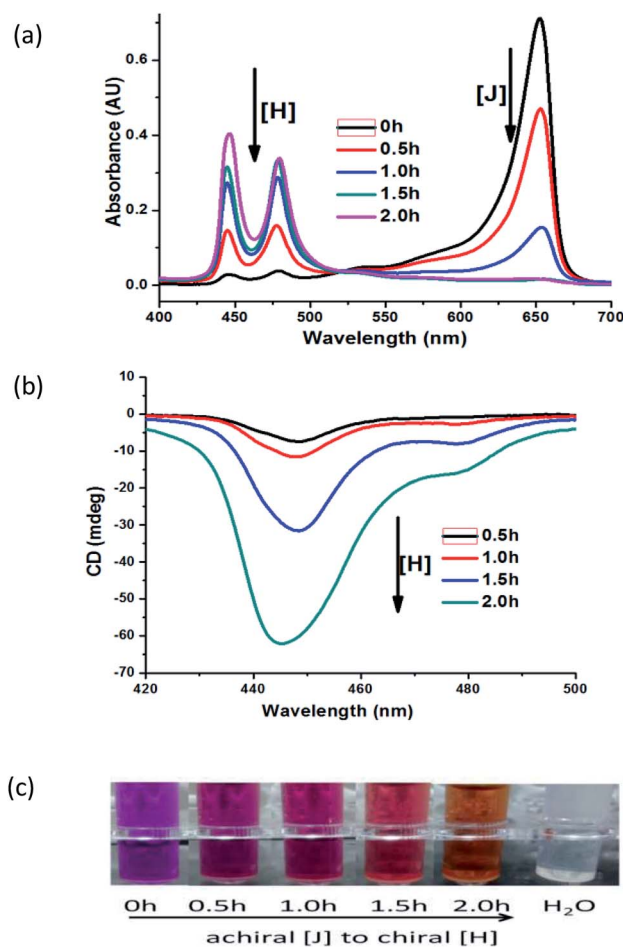


Fig. 2 The transformation from achiral J-aggregates to chiral H-aggregates at room temperature. (a) UV-Vis spectra and (b) CD spectra in 5  $\mu\text{M}$ , all samples were tested after they stood for 2 hours; (c) the solution color changes in 100  $\mu\text{M}$  in 2 hours.

chiral H-aggregates. During the conversion process, the corresponding signals of chiral H-aggregates in 5  $\mu\text{M}$  enhance gradually by UV-Vis (Fig. 2a) and CD spectra (Fig. 2b).

The aggregates of cyanine dyes are very sensitive to external environments, such as solvent, salt, temperature and so on. In our study, we investigated the stability of chiral MTC H-aggregates, which are affected by various temperatures. For the new formation of chiral MTC H-aggregates, they are very stable for several months at room temperature or at 4  $^{\circ}\text{C}$  in the fridge. Even increasing the temperature to 60  $^{\circ}\text{C}$ , the chiral characteristics of MTC H-aggregates in 5  $\mu\text{M}$  could be maintained (Fig. 3). But in high concentration of 100  $\mu\text{M}$ , as the temperature rises, chiral MTC H-aggregates will gradually transform back to achiral J-aggregates. And meanwhile, the transit rate had a positive correlation with the temperature. For example at 50  $^{\circ}\text{C}$ , the chiral H-aggregates transformed to achiral J-aggregates just in five minutes. To our delight, the chiral MTC H-aggregates are restored again when the temperature comes back to room temperature.

It was reported that inorganic salts could promote and accelerate J-aggregation of cyanine dye in water by increasing its effective dielectric constant, and they could also reduce the electrostatic repulsion between dye anions.<sup>13</sup> We are full of curiosity about the effect of NaCl in the formation of chiral MTC H-aggregates. As shown in Fig. 4a, 200  $\mu\text{M}$  MTC methanol solution treated with deionized water without any NaCl presents H-aggregates, with  $\lambda = 531$  nm mainly and a shoulder peak assigned to a monomer state at  $\lambda = 583$  nm, which are achiral. Treated with NaCl aqueous solution at various concentrations, new blue-shifted H-aggregates ( $\lambda = 479$  nm and  $\lambda = 446$  nm) appear, and previously formed H-aggregates ( $\lambda = 531$  nm) and the monomer state ( $\lambda = 583$  nm) disappear gradually. Meanwhile, the increased chiral signals of new formed H-aggregates are confirmed by CD spectra (Fig. 4b). And the high concentration of NaCl could accelerate the formation of chiral H-aggregates, but also bring the precipitation behaviour. Besides NaCl, we also evaluate the influence of KCl and LiCl. KCl had

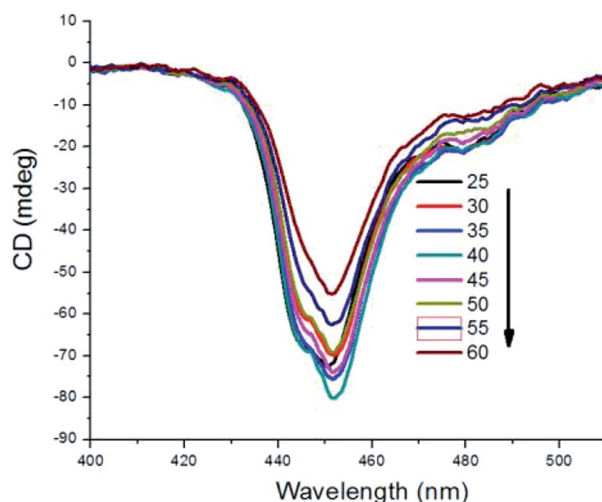


Fig. 3 The stability of MTC chiral H-aggregates in 5  $\mu\text{M}$  at various temperatures monitored by CD spectra, and all samples were tested after they stood for 0.5 hours at designated temperatures.



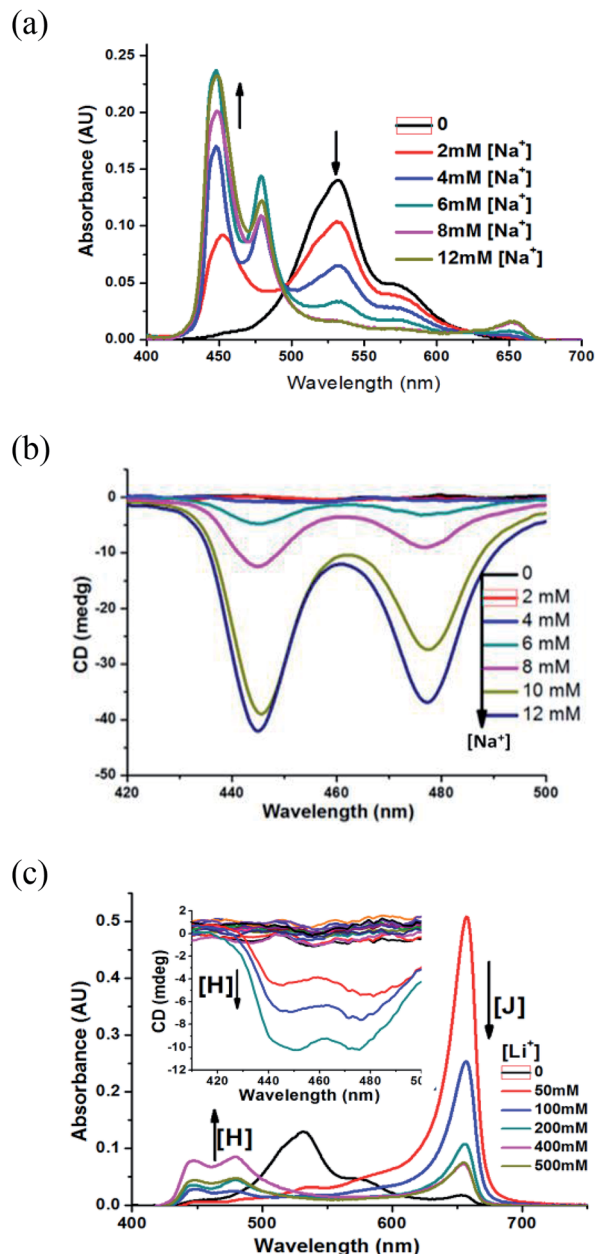


Fig. 4 UV-Vis spectra and CD spectra of MTC self-aggregates in 5  $\mu\text{M}$  dependent on the titration of NaCl (a and b) and LiCl (c), and all samples were tested after they stood for 2 hours at room temperature.

the similar effect on the formation of chiral MTC H-aggregates (Fig. S1<sup>†</sup>). As shown in Fig. 4c, for LiCl in high concentration with the value bigger than 50 mM, it also could induce the formation of chiral MTC H-aggregates. While the concentration of it was lower than 50 mM, just achiral J-aggregates was found (Fig. S2<sup>†</sup>). Upon the addition of LiCl in various concentrations, the conversion from achiral J-aggregates into chiral H-aggregates was obvious slower, maybe attributed to the smaller sizes of lithium ions, which has a much weaker ability to provide asymmetric environments.

The metal salts played a critical role in the formation of chiral MTC H-aggregates, and it is certain that metal salts firstly induce the formation of J-aggregates. The conversion was also

measured by dynamic light scattering (DLS) method to obtain the size distributions of these aggregates. Table 1 summarized the size information for each aggregate including Z-average diameter and major peak diameter. Z-average diameter was used to estimate the size of each aggregate. Achiral J-aggregates had a bigger Z-average 1.95  $\mu\text{m}$ , than the Z-average value for chiral H-aggregates 0.64  $\mu\text{m}$ , obviously.

Transmission electron microscopy (TEM) measurements, as a complementary method, further confirm the structure of chiral H-aggregates macroscopically. The Cryo-Tem micrograph of a 100  $\mu\text{M}$  chiral H-aggregates solution sample is displayed in Fig. 5, and the spiral fibrils can clearly be seen.

It was reported that the role of metal salts was to reduce the electrostatic repulsion between dye anions, thus accelerating the formation of J-aggregates in cyanine dyes.<sup>11,12</sup> While, in our studied system, the achiral J-aggregates could further transform into chiral H-aggregates at room temperature. It was speculated that alkali metal ions listed in different environments for achiral J-aggregates and chiral H-aggregates. First of all, the alkali metal ions replaced its ammonium cations in bigger sizes, and induced the formation of achiral J-aggregates. Then, owing to the presence of propyl sulfonates, the electrostatic interaction between them and alkali metal cations, led to the formation of chiral H-aggregates, showing two absorption of it at 479 and 446 nm, which allows the appearance of the angle  $\alpha$  as shown in the possible model. The possible model for the new formed chiral H-aggregates was proposed (Fig. 6), taking into account the electrostatic interaction between the single dye anions and alkali cations, and the  $\pi/\pi$  interaction between the

Table 1 The particle sizes obtained using DLS for kinds of aggregates in freshly prepared 100  $\mu\text{M}$  solution at room temperature

Aggregate	Z-average (nm)	Peak 1 diameter (nm)	Peak 2 diameter (nm)
Achiral J-aggregates	1951.9	2118.0	95.6
Chiral H-aggregates	642.0	800.4	152.7

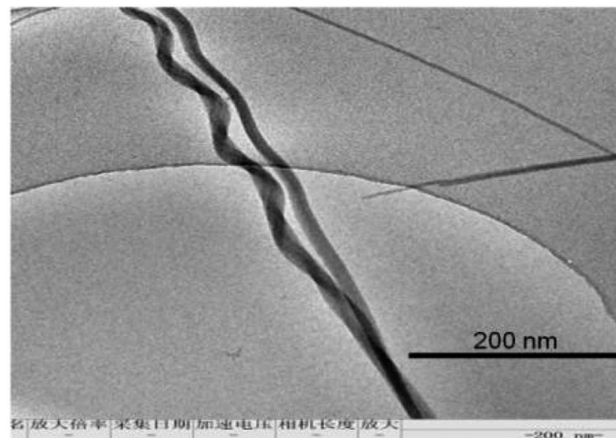


Fig. 5 Cryo-Tem micrograph of a 100  $\mu\text{M}$  chiral H-aggregates solution sample. Bar: 200 nm.





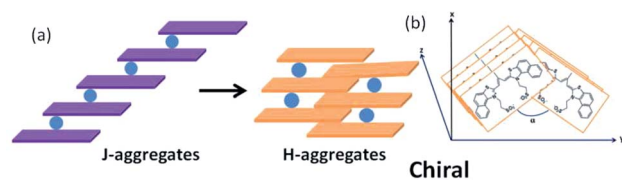


Fig. 6 (a) Schematic illustration of the achiral J-aggregates and chiral H-aggregates. MTC dye molecule: shown as purple or orange cuboid; alkali metal cations are shown as blue balls. (b) Front view of the proposed model structure of chiral H-aggregates.

single dye molecules. Similar structures have been previously proposed for other chiral dye self-aggregates.<sup>6</sup> NMR spectrum indicated that the chemical shift of  $^{23}\text{Na}$  gradually shifted to high field with a smaller value, during the transformation process from achiral J-aggregates to chiral H-aggregates (see Fig. S5†), maybe due to the decreased deshielding effect resulting from the increased space between the two facing dye molecules.

In summary, chiral H-aggregates of a cyanine dye MTC has been investigated. The chiral features of it have been characterized through CD and TEM methods. Chiral H-aggregates can be converted from achiral J-aggregates, and the transformation process have been proved by UV-Vis, CD spectra, and DLS methods, along with the changing solution colours visible to the naked eyes. MTC chiral H-aggregates could be regulated by different alkali metal salts, and thus endows the MTC and its aggregates great advantages in optical application such as molecular probe. Recently, we have made great progress in recognizing some specific DNA and protein structures by achiral cyanine dye aggregates.<sup>14</sup> As is known, biological molecules such as DNA and protein are both chiral and could provide chiral recognition sites, and in our recent research chiral H-aggregates are superior to achiral J-aggregates for recognizing special DNA, owing to their chiral features. The excellently chiral feature of MTC would encourage us to further investigate their aggregation mechanism and application as molecular probe.

## Conflicts of interest

There are no conflicts to declare.

## Acknowledgements

This research was supported under the National Natural Science Foundation of China (Grant No. 21675162, 21472197 and 91027033), the Joint Funds of the National Natural Science Foundation of China (Grant No. U1432250) and “Strategic Priority Research Program” of the Chinese Academy of Sciences (Grant No. XDA09030307).

## References

- 1 M.-H. Liu, L. Zhang and T.-Y. Wang, *Chem. Rev.*, 2015, **115**, 7304.
- 2 (a) A. Abd El-Mageed, M. Handayani, Z. Chen, T. Inose and T. Ogawa, *Chemistry*, Weinheim an der Bergstrasse,

- Germany, 2018; (b) V. Borovkov, *Symmetry*, 2014, **6**, 256; (c) H. Cao and S. De Feyter, *Nat. Commun.*, 2018, **9**, 3416; (d) Z. Chen, Q. Wang, X. Wu, Z. Li and Y.-B. Jiang, *Chem. Soc. Rev.*, 2015, **44**, 4249.
- 3 (a) M. Gaeta, D. Raciti, R. Randazzo, C. Gangemi, A. Raudino, *et al.*, *Angew. Chem., Int. Ed.*, 2018, **57**, 10656; (b) G. Liu, J. Sheng, H. Wu, C. Yang, G. Yang, Y. Li, *et al.*, *J. Am. Chem. Soc.*, 2018, **140**, 6467; (c) G. A. Hembury, V. V. Borovkov and Y. Inoue, *Chem. Rev.*, 2008, **108**, 1; (d) G. Storch and O. Trapp, *Chirality*, 2018, **30**, 1150.
- 4 Y.-H. Shi, H.-X. Sun, J.-F. Xiang, H.-B. Chen, S.-G. Zhang, A.-J. Guan, *et al.*, *Chem. Commun.*, 2016, **52**, 7302, and references cited therein.
- 5 (a) A. Thomas, T. Chervy, S. Azzini, M. H. Li, J. George, C. Genet and T. W. Ebbesen, *J. Phys. Chem. C*, 2018, **122**, 14205; (b) E. Yashima, N. Ousaka, D. Taura, K. Shimomura, T. Ikai and K. Maeda, *Chem. Rev.*, 2016, **116**, 13752; (c) Z. El-Hachemi, O. Arteaga, A. Canillas, J. Crusats, J. Llorens and J. M. Ribo, *Chirality*, 2011, **23**, 585.
- 6 U. D. Rossi, S. Dähne, S. Meskers and H. P. Dekkers, *Angew. Chem., Int. Ed.*, 1996, **35**, 760.
- 7 L.-X. Wang, J.-F. Xiang, H.-X. Sun, Q.-F. Yang, L.-J. Yu, Q. Li, *et al.*, *Dyes Pigm.*, 2015, **122**, 382.
- 8 C. H. G. Williams, *Trans. - R. Soc. Edinburgh*, 1856, **21**, 377.
- 9 (a) B. A. Armitage, *DNA Binders and Related Subjects*, 2005, vol. 253, p. 55; (b) H.-X. Sun, J.-F. Xiang, W. Gai, Y. Liu, A.-J. Guan, *et al.*, *Chem. Commun.*, 2013, **49**, 4510; (c) J. L. Seifert, R. E. Connor, S. A. Kushon, M. Wang and B. A. Armitage, *J. Am. Chem. Soc.*, 1999, **121**, 2987; (d) H.-B. Chen, H.-X. Sun, X. Zhang, X. Sun, Y.-H. Shi and Y.-L. Tang, *RSC Adv.*, 2015, **5**, 1730.
- 10 (a) A. H. Herz, *Adv. Colloid Interface Sci.*, 1977, **8**, 237e98; (b) E. E. Jelley, *Nature*, 1936, **138**, 1009e10; (c) G. Scheibe, *Angew. Chem.*, 1937, **50**, 212e9.
- 11 J.-F. Xiang, X.-R. Yang, C.-P. Chen, Y.-L. Tang, W.-P. Yan and G.-Z. Xu, *J. Colloid Interface Sci.*, 2003, **258**, 198e205.
- 12 Y.-Z. Zhang, J.-F. Xiang, Y.-L. Tang, G.-Z. Xu and W.-P. Yan, *Dyes Pigm.*, 2008, **76**, 88e93.
- 13 B. Robinson, A. Loffler and G. Schwarz, *J. Chem. Soc., Faraday Trans. 1*, 1973, **69**, 56e69.
- 14 (a) Q.-F. Yang, J.-F. Xiang, S. Yang, Q. Li, Q.-J. Zhou, A.-J. Guan, *et al.*, *Anal. Chem.*, 2010, **82**, 9135e7; (b) Q.-F. Yang, J.-F. Xiang, S. Yang, Q. Li, Q.-J. Zhou, A.-J. Guan, *et al.*, *Nucleic Acids Res.*, 2010, **38**, 1022e33; (c) W. Gai, Q.-F. Yang, J.-F. Xiang, W. Jiang, Q. Li, H.-X. Sun, *et al.*, *Nucleic Acids Res.*, 2013, **41**, 2709e22; (d) L.-J. Yu, Q.-F. Yang, J.-F. Xiang, H.-X. Sun, L.-X. Wang, Q. Li, *et al.*, *Analyst*, 2015, **140**, 1637e46; (e) B. Liu, Z.-H. Wang, L. Lan, Q.-F. Yang, P.-P. Zhang, L. Shi, *et al.*, *Chem.-Eur. J.*, 2018, **24**, 6727; (f) Y.-H. Wu, H. Zhang, J.-F. Xiang, Z.-H. Mao, G. Shen, F.-M. Yang, *et al.*, *Talanta*, 2018, **179**, 501; (g) G. Shen, H. Zhang, C.-R. Yang, Q.-F. Yang and Y.-L. Tang, *Anal. Chem.*, 2017, **89**, 548; (h) S.-J. Xu, Q. Li, J.-F. Xiang, Q.-F. Yang, H.-X. Sun, A.-J. Guan, *et al.*, *Nucleic Acids Res.*, 2015, **43**, 9575.

